Redox Regulation of SH2-Domain-Containing Protein Tyrosine Phosphatases by Two Backdoor Cysteines

Cheng-Yu Chen,[‡] Devina Willard,[‡] and Johannes Rudolph*,[§]

Department of Chemistry and Biochemistry, University of Colorado, Boulder, Colorado 80309, and Department of Biochemistry, Duke University, Durham, North Carolina 27710

Received October 21, 2008; Revised Manuscript Received December 22, 2008

ABSTRACT: Protein tyrosine phosphatases (PTPs) are known to be regulated by phosphorylation, localization, and protein−protein interactions. More recently, redox-dependent inactivation has emerged as a critical factor in attenuating PTP activity in response to cellular stimuli. The tandem Src homology 2 domain-containing PTPs (SHPs) belong to the family of nonreceptor PTPs whose activity can be modulated by reversible oxidation in vivo. Herein we have investigated in vitro the kinetic and mechanistic details of reversible oxidation of SHP-1 and SHP-2. We have confirmed the susceptibility of the active site cysteines of SHPs to oxidative inactivation, with rate constants for oxidation similar to other PTPs (2−10 M^{-1} s^{-1}). Both SHP-1 and SHP-2 can be reduced and reactivated with the reductants DTT and gluthathione, whereas only the catalytic domain of SHP-2 is subject to reactivation by thioredoxin. Stabilization of the reversible oxidation state of the SHPs proceeds via a novel mechanism unlike for other PTPs wherein oxidation yields either a disulfide between the catalytic cysteine and a nearby "backdoor" cysteine or a sulfenylamide bond with the amide backbone nitrogen of the adjacent amino acid. Instead, in the reversibly oxidized and inactivated SHPs, the catalytic cysteine is rereduced while two conserved backdoor cysteines form an intramolecular disulfide. Formation of this backdoor−backdoor disulfide is dependent on the presence of the active site cysteine and can proceed via either active site cysteine−backdoor cysteine intermediate. Removal of both backdoor cysteines leads to irreversible oxidative inactivation, demonstrating that these two cysteines are necessary and sufficient for ensuring reversible oxidation of the SHPs. Our results extend the mechanisms by which redox regulation of PTPs is used to modulate intracellular signaling pathways.

Protein tyrosine phosphatases (PTPs)[1] are important mediators of multiple signaling pathways in essential cellular processes such as proliferation, differentiation, and migration. Like other key signaling proteins, PTPs are highly regulated by various mechanisms including interactions with other proteins, phosphorylation levels, and intracellular localization. Recently, there has been increasing evidence demonstrating a more primary mode for regulation of PTP activity involving reversible oxidation by reactive oxygen species (ROS) such as hydrogen peroxide (H_2O_2) (*1*−*4*). Extracellular stimuli including hormones, growth factors, and cytokines induce activation of cell surface receptors, which, in addition to the primary response (e.g., receptor dimerization and downstream signaling), can lead to production of intracellular ROS to concentrations as high as 0.1−1 mM (*5, 6*). These ROS readily oxidize cysteine thiolate anions ($Cys\text{-}S^-$), in particular the catalytic cysteines found in the active sites of all PTPs. Intracellular ROS thus promote signaling events dependent on the inactivation of PTPs.

The tandem SH2 (Src homology 2 domain) containing PTPs (SHPs) are among the increasing number of PTPs for which ROS-mediated redox regulation has been implicated. The SHPs, including SHP-1 and SHP-2 in humans, are characterized by two N-terminal SH2 domains, a catalytic PTP domain, and an inhibitory C-terminus (*7*−*9*). SHP-1 and SHP-2 perform opposing tasks in signaling pathways. SHP-1, predominantly expressed in hematopoetic cells, is a negative regulator in the signaling pathways mediated by the chemokine and cytokine receptors and other receptor tyrosine kinases. The more widely expressed SHP-2 is a positive regulator in signaling pathways mediated by numerous receptor tyrosine kinases, the Ras-extracellular signal-regulated kinase, the T-cell receptor, and the cytokine receptor signaling pathways. Despite their opposite roles in signaling there is considerable evidence that both SHP-1 and SHP-2 are regulated by reversible oxidation. For SHP-1, in T-cells treated with hydrogen peroxide, redox-mediated inhibition of SHP-1 leads to increased phosphorylation of downstream substrates such as the ERK and p38 but not JNK kinases (*10*). For SHP-2, stimulation of T-cell receptors by T-cell antigen leads to production of H_2O_2, reversible oxidation of SHP-2, increased phosphorylation of its down-

* To whom correspondence should be addressed: phone, (303) 492-3545; fax, (303) 954-9550; e-mail, jrudolph@colorado.edu.

[‡] Duke University.

[§] University of Colorado.

[1] Abbreviations: PTP, protein tyrosine phosphatase; ROS, reactive oxygen species; SH2, Src homology 2 domain; SHP, SH2-domain containing PTP; ΔSHP-1, catalytic domain of SHP-1 (residues 247−514); ΔSHP-2, catalytic domain of SHP-2 (residues 268−525); MKP3, mitogen-activated protein kinase phosphatase 3; DTT, dithiothreitol; GSH, glutathione; TR/TRR, thioredoxin/thioredoxin reductase; MALDI-MS, matrix-assisted laser desorption ionization mass spectrometry; IAA, iodoacetic acid; mFP, 3-*O*-methylfluorescein phosphate.

10.1021/bi801973z CCC: $40.75
Published on Web 01/23/2009

stream substrates, and integrin activation (*11*). Signal transduction and induction of mitogenesis through the platelet-derived growth factor receptor has also been shown to depend on transient oxidation of SHP-2 (*12*). Most recently, reversible oxidation of SHP-2 has been found subsequent to stimulation of cells with epidermal growth factor, playing a critical role in fibroblast proliferation and subsequent cardiac fibrosis (*13*).

Despite having diverse sequences and protein folds, all cysteine-based phosphatases including the PTPs, dual-specificity phosphatases (DSPs), and low molecular weight phosphatases contain a catalytic cysteine in a highly conserved active site motif (H-C-X_5-R; single amino acid code wherein X represents any amino acid). Unlike a typical protonated cysteine thiol (pK_a $\sim$ 8.5), such a catalytic cysteine has a pK_a that is perturbed to the acidic range (4.5−7), favoring formation of a thiolate anion (Cys-S^-) under physiological conditions (*14*). Oxidation of this reactive catalytic cysteine yields a reversibly oxidized sulfenic acid (Cys-SO^-) that is susceptible to further irreversible oxidation to the sulfinic (Cys-SO_2^-) or sulfonic (Cys-SO_3^-) species. Because the inactive yet reversibly oxidized enzyme serves as a switch in controlling signaling pathways, cysteine-based phosphatases have evolved mechanisms to preserve the reversible oxidation state of the sulfenic acid. For many phosphatases, including the low molecular weight phosphatases (LMW) (*15*), the cell cycle Cdc25 phosphatases (*16*−*19*), phosphatase and tensin homologue (PTEN) (*20*), and kinase associated phosphatase (KAP) (*21*), biochemical and/or structural studies have shown that the reversibly inactivated state is stabilized by formation of an intracellular disulfide bond between the active site cysteine and a nearby "backdoor" cysteine. In contrast, for PTP1B (*22, 23*) and PTPα (*24*), the initial oxidation of the active site cysteine is trapped as a reversible sulfenylamide bond to the adjacent amino acid. The disulfide and sulfenylamide bonds are resistant to further oxidation under physiological levels of ROS and can be rereduced to the active thiolate by reductants such as dithiothreitol (DTT), glutathione (GSH), and/or thioredoxin/thioredoxin reductase (TR/TRR).

Both SHP-1 and SHP-2 share the characteristic active site motif (H-C-X_5-R) and conserved catalytic cysteine of all PTPs. In addition to sharing a similar protein fold with PTP1b, both SHP-1 and SHP-2 have the same five variable X residues in the active site loop as PTP1b (S-A-G-I-G). Titration of the active site of SHP-1 using aromatic disulfides suggests that the catalytic cysteine in SHP-1 has a low pK_a compared to other cysteines in the protein (*25*). In addition, S-nitrosylation of the catalytic cysteine has been reported to inhibit the phosphatase activity of SHP-1 in vivo (*26*). Thus, as for other PTPs, the catalytic cysteines in the SHPs appear susceptible to oxidation by ROS. There appear to be several possible mechanisms for protecting the initial sulfenic acid from further irreversible oxidation in the SHPs. Based on the similarity in the active site pocket to PTP1b and PTPα, sulfenylamide formation with the downstream amide nitrogen is possible. Alternatively, based on the proximity of two highly conserved cysteines seen in the structures of SHP-1 (*27*) and SHP-2 (*28*), formation of intramolecular disulfides also seems to be possible. The two potential backdoor cysteines are located 9 to 12 Å from the catalytic cysteine, within the range observed for PTPs and dual-specificity phosphatases known to use a disulfide for protecting against irreversible oxidation. Toward a better understanding of the molecular mechanism for the oxidative regulation of the SHPs, we investigated herein their oxidation by hydrogen peroxide and reactivation by different reductants (DTT, GSH, and TR/TRR), with particular emphasis on the role of the two potential backdoor cysteines. Our results demonstrate transient formation of a sulfenic acid at the active site followed by formation of an inactive and reversibly oxidized form wherein the catalytic cysteine is rereduced and the two backdoor cysteines are oxidized to form an intramolecular disulfide.

MATERIALS AND METHODS

Materials. Hydrogen peroxide (H_2O_2) was purchased from EM Science and dilutions to 1 M were prepared fresh daily. Thioredoxin/thioredoxin reductase (TR/TRR) from *Escherichia coli* was a generous gift from JoAnne Stubbe (Massachusetts Institute of Technology, Cambridge, MA). NADPH, mFP, DTT, IAA, glutathione, and catalase were obtained from Sigma. Sequencing-grade trypsin was purchased from Promega and was dissolved in 50 mM acetic acid. Pfu DNA polymerase was obtained from Stratagene. Restriction enzymes were obtained from New England BioLabs. Cloning vectors pET28a and pET30 a were obtained from Novagen.

Cloning, Expression, and Purification of Full-Length SHP-1 and SHP-2. The open reading frames of full-length SHP-1 and SHP-2 were amplified from a cDNA library derived from human brain by PCR (cycle 1, 95 °C, 3 min, 55 °C, 1.5 min, 72 °C, 2.75 min; cycles 2−41, 95 °C, 1 min, 53 °C, 1.5 min, 72 °C, 2.75 min; final cycle, 72 °C, 8 min) using the primers TATACATATGCTGTCCCGTGGGTGGTTTCACCG and TATAGAATTCTCACTTCCTCTTGAGGGAACCCTTGC for SHP-1 and ATATACATATGACATCGCGGAGATGGTTTCACCC and ATATAGAATTCTCATCTGAAACTTTTCTGCTGTTGC for SHP-2. After digestion of the PCR products with *Nde*I and *Eco*RI, SHP-1 and SHP-2 were cloned into the pET30a expression vector and transformed into *E. coli* BL21(DE3) cells for expression. The proteins were expressed by induction of midlog cells with 0.2 mM IPTG overnight at 25 °C. In a typical preparation, 30 g of frozen cell pellets was thawed in 60 mL of buffer A (20 mM MES, pH 5.5, 1 mM EDTA, and 1 mM DTT) supplemented with protease inhibitor cocktail from Boehringer Mannheim. The cells were lysed by sonication, and cell debris was removed by centrifugation at 20000*g* for 30 min. The resulting supernatant was bound to SP-Sepharose (7 mL) equilibrated in buffer A. The column was washed extensively with buffer A, and the proteins were eluted with a linear gradient of NaCl (0−0.5 M) in buffer A. Fractions containing PTP activity were combined, concentrated with an Amicon YM10 concentrator, and exchanged into buffer B (50 mM Tris, pH 8.5, 1 mM EDTA, and 1 mM DTT) by multiple dilutions and reconcentrations. Proteins were then bound to Q-Sepharose (5 mL) equilibrated in buffer B. SHPs were eluted with a linear gradient of NaCl (0 to 0.5 M) in buffer B and further purified by Superdex-200 chromatography in TNED buffer (50 mM Tris-HCl, pH 7.5, 50 mM NaCl, 1 mM EDTA, and 1 mM DTT). The purified proteins (>90% pure by SDS−PAGE) were con-

Scheme 1: Reaction Pathway for Oxidation/Reduction of the SHPs[a]

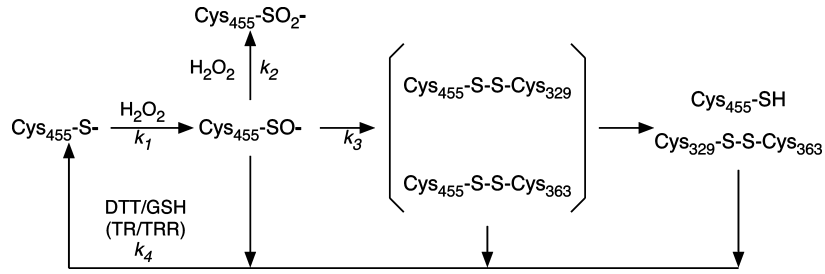

[a] The kinetic and mechanistic reaction pathway for oxidation and rereduction of the SHPs is outlined using SHP-1 as an example. Initial oxidation of the active site Cys455 by hydrogen peroxide ($k_1[H_2O_2]$) yields the sulfenic acid. Further oxidation ($k_2[H_2O_2]$) would yield higher oxidation species such as the sulfonic acid. Instead, rapid intramolecular disulfide ($k_3 > k_2[H_2O_2]$) formation with one of two backdoor cysteines (Cys329 or Cys363) followed by disulfide exchange yields the stable backdoor−backdoor disulfide. Rereduction of either the sulfenic acid or any of the disulfides yields active enzyme (k_4[reductant]). Measured atomic distances ($\gamma S-\gamma S$) from the crystal structures of SHP-1 (PDB ID 1gwz) and SHP-2 (PDB ID 2shp) are as follows: SHP-1, C363−C455 = 9.43 Å, C329−C455 = 12.35 Å, and C329−C363 = 5.32 Å; SHP-2, C367−C459 = 9.66 Å, C333−C459 = 12.40 Å, and C333−C367 = 5.07 Å.

centrated to 10 mg/mL using an Amicon Ultra-15 concentrator with addition of glycerol (10% final) and frozen in liquid N_2 for storage at −80 °C.

Cloning, Expression, and Purification of Catalytic Domains of SHP-1 and SHP-2. The His-tagged catalytic domains of SHP-1 (ΔSHP-1, residues 247−514) and SHP-2 (ΔSHP-2, residues 268−525) were PCR amplified (cycle 1, 95 °C, 3 min, 55 °C, 1.5 min, 72 °C, 2 min; cycles 2−31, 95 °C, 1 min, 55 °C, 1.5 min, 72 °C, 2 min; final cycle, 72 °C, 5 min) from the full-length clones using the primers CCCATATGGGCTTCTGGGAGGAGTTTGAGAG and ACAAGCTTCACTTCTGCGACTGCAGGACCTC for ΔSHP-1 and GACATATGGGTCAAAGGCAAGAAAACAAAAAC and TCAAGCTTCATAGTGTTTCAATATAATGCTG for ΔSHP-2. After digestion of the PCR products with *Nde*I and *Hin*dIII, ΔSHP-1 and ΔSHP-2 were cloned into the pET28a expression vector and transformed into *E. coli* BL21(DE3) cells for expression. Following induction as for the full-length proteins, the cleared cell lysates were incubated with Ni-NTA agarose (5 mL) in buffer C (50 mM Tris, pH 8.0, and 250 mM NaCl). The agarose was washed extensively with buffer C containing 20 mM imidazole. The His-tagged proteins were eluted with 500 mM imidazole and further purified by Superdex-75 gel chromatography in TNED buffer. The purified proteins (>90% pure by SDS−PAGE) were concentrated to >20 mg/mL using an Amicon Ultra-15 concentrator with addition of glycerol (10% final) and frozen in liquid N_2 for storage at −80 °C. Various cysteine mutants were generated by Quick-Change mutagenesis (Stratagene) according to the manufacturer's instructions using the following primers for ΔSHP-1, C363S, GGCCGGAACAAATCCGTCCCATACTGG and CCAGTATGGGACGGATTTGTTCCGGCC; C329S, ATCGCCAGCCAGGGCTCTCTGGAGGCCACGGTC and GACCGTGGCCTCCAGAGAGCCCTGGCTGGCGAT; C455S, CCATCATCGTGCACTCCAGCGCCGGCATC and GATGCCGGCGCTGGAGTGCACGATGATGG; and for ΔSHP-2, C333S, ATTGCCACACAAGGCTCCCTGCAAAACACGGTG and CACCGTGTTTTGCAGGGAGCCTTGTGTGGCAAT; C367S, AGAGGAAAGAGTAAATCTGTCAAATACTGGCCT and AGGCCAGTATTTGACAGATTTACTCTTTCCTCT. The C363S/C329S double mutation of ΔSHP-1 was generated from the single mutant ΔSHP-1 (C363S) with use of the C329S primers. The mutant proteins were purified as described for the wild-type catalytic domains.

Rate of Inactivation by H_2O_2. The rate of inactivation of SHPs was calculated using a fixed time-point quench protocol. SHPs (100−200 μM) were incubated at 25 °C with varying concentrations of H_2O_2 (1−5 mM) in buffer H (50 mM HEPES, pH 7.5, 100 mM NaCl, and 1 mM EDTA) for the full-length enzymes and in 3C buffer (50 mM Tris, 50 mM bis-Tris, and 100 mM sodium acetate, pH 7.5) for the catalytic domains. At varying time points (30 s to 15 min), aliquots were taken and diluted (200-fold) into 3C buffer containing 10 units of catalase. Phosphatase activities were measured immediately using 3-*O*-methylfluorescein phosphate (mFP; 250 μM) in a continuous assay that monitors product formation at 477 nm ($\epsilon = 27200\ M^{-1}\ cm^{-1}$). The percent remaining activities were determined by comparison with mock-treated samples. The observed rate constant of inactivation (k_{obs}) was determined by fitting with the equation:

$$\%\ \text{remaining activity} = 100e^{-k_{obs}t} + \text{residual activity} \quad (1)$$

The second-order rate constant k_1 (Scheme 1) was obtained by fitting the linear dependence of the rate of inactivation (k_{obs}) on the concentration of H_2O_2.

Rate of Reactivation by DTT, GSH, and TR/TRR. The SHPs (100 − 200 uM) were initially inactivated by incubation with H_2O_2 (0.5 − 2 mM) for 10 to 15 min. Aliquots were then diluted 2-fold into buffer H (for full-length SHPs) or 3C buffer (for catalytic domains) containing 10 units of catalase and varying amounts of DTT (10− 200 mM), GSH (50−200 mM), or TR/TRR (0.2−5 equivalents of TR to SHP enzyme). Following incubation under reducing conditions for varying amounts of time (20 s − 10 min), aliquots were diluted 100-fold into 3C buffer and phosphatase activity was measured using mFP (250 μM). When using TR/TRR as the reductant, NADPH (16 − 400 uM) was also included and the ratio of TR to TRR was held fixed at 200 to 1. Control experiments verified that catalase was not required for reactivation using DTT or GSH because even the lowest concentration of reductant was sufficient for rapidly inactivating all H_2O_2. The observed rate constant of reactivation (k_{react}) was determined by fitting with the equation:

$$\%\ \text{recovered activity} = 100(1 - e^{-k_{obs}t}) + \text{residual activity} \quad (2)$$

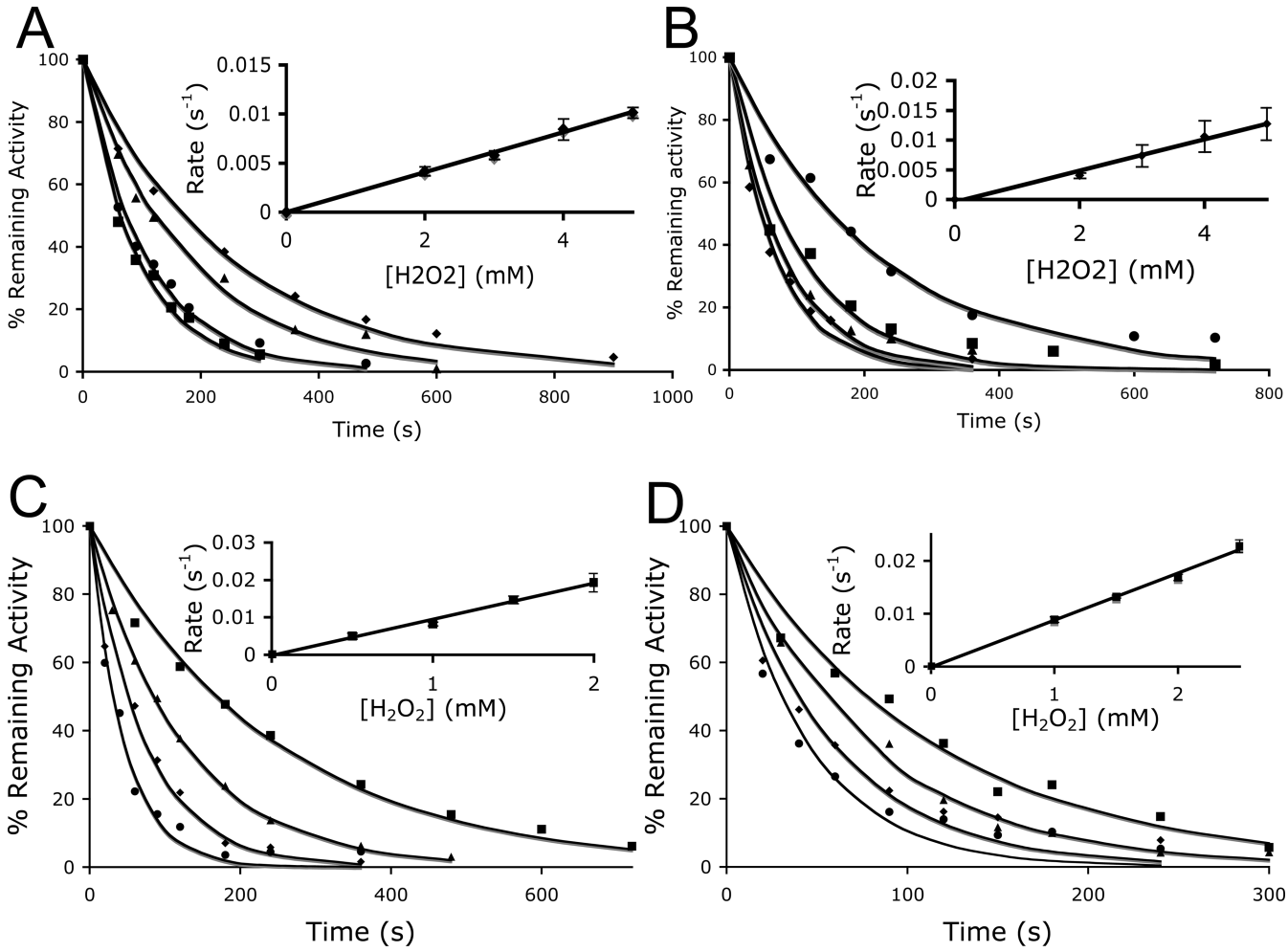

FIGURE 1: Time-dependent inactivation of SHPs by H_2O_2. (A) Full-length SHP-1 at concentrations of H_2O_2: 2.0 mM (◆), 3.0 mM (▲), 4.0 mM (●), and 5.0 mM (□). In the inset, the concentration dependence of the rate of inactivation was used to derive a second-order rate constant, k_1, of 2.0 M^{-1} s^{-1}. (B) Full-length SHP-2 at concentrations of H_2O_2: 2.0 mM (●), 3.0 mM (□), 4.0 mM (▲), and 5.0 mM (◆). The inset yields a second-order rate constant of k_1 of 2.4 M^{-1} s^{-1}. (C) The catalytic domain ΔSHP-1 at concentrations of H_2O_2: 0.5 mM (□), 1.0 mM (▲), 1.5 mM (◆), and 2.0 mM (●). The inset yields a second-order rate constant of k_1 of 9.4 M^{-1} s^{-1}. (D) The catalytic domain ΔSHP-2 at concentrations of H_2O_2: 1.0 mM (□), 1.5 mM (▲), 2.0 mM (◆), and 2.5 mM (◆). The inset yields a second-order rate constant of k_1 of 8.8 M^{-1} s^{-1}.

The second-order rate constant k_4 (Scheme 1) was obtained by fitting the linear dependence of the rate of reactivation (k_{react}) on the concentration of reductants.

MALDI-MS Spectrometry. Samples for matrix-assisted laser desorption mass spectrometry (MALDI-MS) were prepared by incubating SHPs (~50 μg) with or without H_2O_2 followed by 10-fold dilution into 50 mM ammonium bicarbonate buffer at pH 7.8. Excess H_2O_2 was then rapidly removed by a G-25 spin column. To prevent disulfide exchange during the subsequent workup, remaining free cysteines were blocked by reaction for 30 min with iodoacetic acid (IAA; 50 mM). Remaining iodoacetic acid was removed by a G-25 spin column. The SHPs were then digested with 0.5 μg of sequencing grade trypsin by incubation overnight at 37 °C. The digested peptide mixture was desalted with a C_{18}-ZipTip (Millipore) and analyzed by MALDI-TOF using a Voyager DE-Pro.

RESULTS

Inactivation of Full-Length SHPs and the Catalytic Domain of SHPs by H_2O_2. In vivo studies have demonstrated the inactivation of SHP phosphatase activity in response to external H_2O_2 or growth factor stimulated production of H_2O_2. Additionally, preliminary studies in vitro have indicated that oxidation of SHP-1 is readily reversible (*29*). However, no evidence has been found that this inactivation is a result of direct oxidation of the active site cysteine in the SHPs. We began this study by determining the susceptibility of SHP-1 and SHP-2 to oxidative inactivation in vitro. In our studies we used both full-length SHPs and their catalytic domain constructs (ΔSHP-1 and ΔSHP-2). The catalytic domains reflect activated SHPs wherein the SH2 domains are disengaged from the active sites, instead binding to specific pTyr motifs in receptor tyrosine kinases (*30, 31*). By measuring remaining phosphatase activity as a function of time and concentration of H_2O_2, we determined the second-order rate constants for oxidation of the SHPs (Scheme 1, Figure 1, Table 1). SHP-1 and SHP-2 showed similar rate constants for oxidation by H_2O_2 (2.0 and 2.4 M^{-1} s^{-1}, respectively), as expected from their similar active sites. In comparison, the rate constants for inactivation of ΔSHP-1 and ΔSHP-2 are ~4-fold higher than for the full-length proteins (9.4 and 8.8 M^{-1} s^{-1}, respectively). Slower oxidation for the full-length SHPs is consistent with their

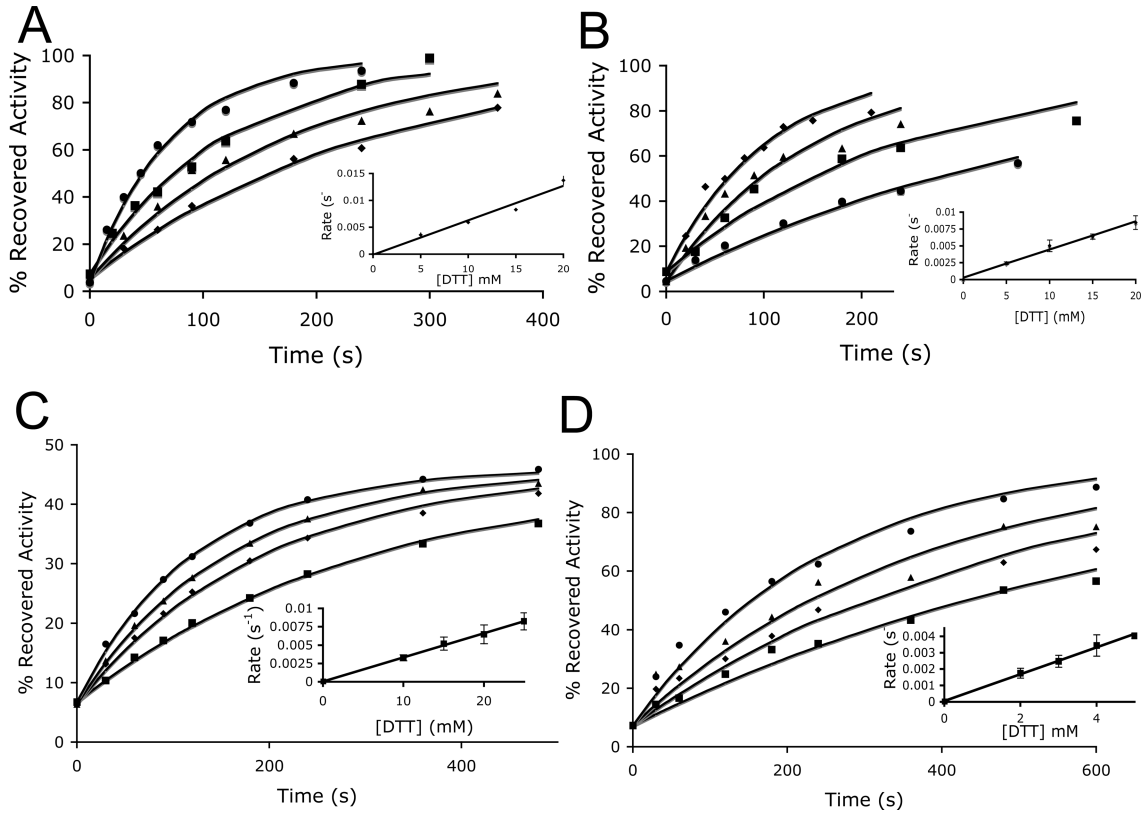

FIGURE 2: Time-dependent reactivation of SHPs by DTT. (A) SHP-1 at concentrations of DTT: 5 mM (◆), 10 mM (▲), 15 mM (□), and 20 mM (●). The inset yields a second-order rate constant of k_4 of 0.64 M^{-1} s^{-1}. (B) SHP-2 at concentrations of DTT: 5 mM (●), 10 mM (□), 15 mM (▲), and 20 mM (◆). The inset yields a second-order rate constant of k_4 of 0.46 M^{-1} s^{-1}. (C) ΔSHP-1 at concentrations of DTT: 10 mM (□), 15 mM (◆), 20 mM (▲), and 25 mM (●). The inset yields a second-order rate constant of k_4 of 0.33 M^{-1} s^{-1}. (D) ΔSHP-2 at concentrations of DTT: 2 mM (□), 3 mM (◆), 4 mM (▲), and 5 mM (●). The inset yields a second-order rate constant of k_4 of 0.84 M^{-1} s^{-1}.

Table 1: Rate Constants of Oxidation and Reactivation for SHP-1 and SHP-2

enzyme	k_1 (H_2O_2) (M^{-1} s^{-1})	k_4 (DTT) (M^{-1} s^{-1})	k_4 (GSH) (M^{-1} s^{-1})	k_4 (TR/TRR) (M^{-1} s^{-1})
SHP-1	2.0 ± 0.1	0.64 ± 0.08 (87 ± 8%)[b]	0.026 ± 0.003 (97 ± 2%)	nd[a]
SHP-2	2.4 ± 0.3	0.46 ± 0.04 (88 ± 3%)	0.16 ± 0.04 (96 ± 3%)	nd[a]
ΔSHP-1	9.4 ± 0.8	0.33 ± 0.01 (46 ± 3%)	0.077 ± 0.014 (65 ± 1%)	nd[a]
ΔSHP-2	8.8 ± 0.3	0.84 ± 0.03 (88 ± 3%)	0.07 ± 0.01 (100 ± 10%)	36.5 ± 2.1 (86 ± 8%)
ΔSHP-1 (C329S)	9.6 ± 1.4	0.16 ± 0.03 (86 ± 8%)	0.053 ± 0.008 (86 ± 3%)	nd[a]
ΔSHP-1 (C363S)	6.5 ± 0.2	0.77 ± 0.05 (48 ± 4%)	0.092 ± 0.013 (53 ± 5%)	nd[a]
ΔSHP-1 (C363S/C329S)	1.1 ± 0.1	nd[a]	nd[a]	nd[a]

[a] Not detectable. [b] Percent of recovered activity compared to mock inactivation/reactivation was derived from the maximum phosphatase activity recovered after treatment with reductants.

reported lower phosphatase activity, wherein the N-terminal SH2 domain interacts with and alters the conformation of the catalytic pocket (*28, 32*). The more rapid oxidative inactivation for the catalytic domains of the SHPs suggests that oxidation targets the catalytic cysteine. The inactivation rates for the catalytic domains of the SHPs are comparable to the rates of inactivation rates for other phosphatases implicated in regulation by direct oxidation including PTP1b (9.1 M^{-1} s^{-1} (*33*)), VHR (17.9 M^{-1} s^{-1} (*33*)), and mitogen-activated protein kinase phosphatase (MKP3; 9.6 M^{-1} s^{-1} (*34*)) but slower than for Cdc25B (164 M^{-1} s^{-1} (*17*)).

Reactivation of the SHPs by DTT, GSH, and TR/TRR. We next characterized the rereduction and concomitant reactivation of the SHPs by different reductants including DTT, glutathione (GSH), and thioredoxin/thioredoxin reductase (TR/TRR). Each SHP was first inactivated under appropriate specific conditions to yield less than 5% remaining activity and then quenched into buffer containing varying amounts of catalase and/or reducing agent. After further incubation to allow rereduction of the catalytic cysteine, the recovery of activity was measured as a function of time and concentration of reductant (Scheme 1). The rate of reactivation varied linearly as a function of reductant (Figure 2, Table 1). For SHP-1, SHP-2, and ΔSHP-2, more than 80% activity was recovered with both DTT and GSH, while ~50% was recovered for ΔSHP-1. Only ΔSHP-2 could be reactivated with TR/TRR (36.5 ± 2.1 M^{-1} s^{-1}). The inability to reduce ΔSHP-1 with TR/TRR hints at a potential physiological difference in the regulation of SHP-1 and SHP-2.

Identification of the Backdoor Cysteine Residues in the Catalytic Domain of the SHPs. Recovery of high levels of activity following oxidation and subsequent reduction for the SHPs (Table 1) and the known reactivity of sulfenic acids (*35*) implied the existence of a protective mechanism to prevent irreversible oxidation of the catalytic cysteines (Scheme 1). Given the presence of two conserved potential

backdoor cysteines, we focused on the possible formation of intramolecular disulfide bonds using MALDI-MS. To reflect the active form of the enzyme and simplify the spectra, we chose to study the catalytic domain alone. To prevent disulfide exchange during the analysis, all samples were treated with 50 mM iodoacetic acid prior to workup for MALDI-MS, thus trapping free cysteines in the carboxymethylated form but not modifying disulfides or oxidized cysteines. As expected for the nonoxidized forms of ΔSHP-1 and ΔSHP-2, we identified the active site peptides containing the carboxymethylated catalytic cysteines: QESLPHAGPIIVHC*SAGIGR in ΔSHP-1 at 2101 Da and QESIMDAGPVVVHC*SAGIGR in ΔSHP-2 at 2086 Da (Figure 3). Additionally, we observed the peptides containing the carboxymethylated backdoor cysteine residues (Figure 3). Therefore, no intramolecular disulfides exist in the reduced catalytic domains of either phosphatase. Following oxidation to a rereducible form, we expected to find the catalytic cysteines as sulfenic acids or in a disulfide bonds with one of the potential backdoor cysteines. We were thus surprised to identify the same tryptic peptides containing the carboxymethylated catalytic cysteines in the oxidized samples of both ΔSHP-1 and ΔSHP-2 (Figure 3). The MALDI spectra from the oxidized ΔSHPs did contain a novel fragment not seen in the reduced samples, which corresponded to a disulfide linkage between the two potential backdoor cysteines (4515 Da for ΔSHP-1, 2465 for ΔSHP-2; Figure 3). Appearance of these backdoor−backdoor disulfides was accompanied by the significant reduction in the intensity of the individual peaks representing the carboxymethylated backdoor cysteines for ΔSHP-1 (Figure 3A).

To ensure that disulfide formation between the two backdoor cysteines did not occur directly but instead depended on prior oxidation of the active site cysteine, we next generated the active site mutant C455S of ΔSHP-1. As expected, the mutant protein had no detectable phosphatase activity with the substrate mFP. Using MALDI-MS, C455S yielded the active site peptide with a serine mutation (2028 Da) and the same two peptides containing the carboxymethylated backdoor cysteines (1523 and 3108 Da, Figure 3C), even following oxidation by H_2O_2. The lack of an intramolecular disulfide between the two backdoor cysteines in the absence of the catalytic cysteine indicates that oxidation of the catalytic cysteine is a prerequisite to formation of the backdoor−backdoor disulfide. Consistent with this interpretation, the MALDI-MS spectrum of oxidized ΔSHP-1 shows molecular masses that correspond to the active site peptide with the sulfenic acid (∼2059) and sulfinic acid (∼2076 Da) modifications (Figure 3A, blown-up region). The detection of the sulfenic acid-containing peptide is consistent with the expected intermediate on the path to disulfide formation (Scheme 1). The detection of the sulfinic acid-containing peptide is consistent with the incomplete reversibility of oxidative inactivation for ΔSHP-1 (Table 1). The absence of a sulfenic acid intermediate or sulfinic acid byproduct following oxidation of ΔSHP-2 presumably reflects the greater efficiency of transfer of the oxidation state from the active site cysteine to the two backdoor cysteines (Scheme 1) and is consistent with the high recovery of activity upon subsequent reduction (Table 1).

Identification of Disulfide Intermediates by Mutagenesis of the Backdoor Cysteines. To explain the mechanism by which we obtain a reduced catalytic cysteine and a backdoor−backdoor cysteine disulfide as the stable end product of oxidation, we hypothesized that the catalytic cysteine, following initial oxidation to the sulfenic acid, first forms a transient disulfide with one or the other of the two backdoor cysteines (Scheme 1). The proximity (<6 Å) of the two backdoor cysteines to each other would then favor formation of the backdoor−backdoor disulfide. We used site-directed mutagenesis and MALDI-MS to probe this mechanism, wherein mutation of one of the backdoor cysteines could yield a disulfide between the catalytic cysteine and the remaining backdoor cysteine, representing a disulfide intermediate during the process of oxidation of the wild-type protein. Alternatively, removing both backdoor cysteines could lead to irreversible inactivation wherein disulfide exchange is no longer possible and the catalytic cysteine becomes oxidized to the sulfinic or sulfonic acid. We first mutated the backdoor cysteines that are further from the catalytic cysteine, namely, Cys329 in ΔSHP-1 and Cys333 in ΔSHP-2. The C329S mutant showed similar activity as wild-type ΔSHP-1, while the C333S mutant had less than 10% activity as compared to wild-type ΔSHP-2. Because the reduced activity of Cys333 in ΔSHP-2 may reflect a significant perturbation in the overall structure of the protein or a change in the microenvironment of the active site, we focused on characterizing the redox reactions of the C329S mutant of ΔSHP-1.

Purified C329S was treated with the same oxidation and reduction conditions as the wild-type protein. The C329S mutant had similar rate constants for oxidation and reactivation as the wild-type protein, indicating that the C329S mutation does not affect the chemical environment of the catalytic cysteine (Table 1). To probe the mechanism by which C329S achieves a reversibly oxidized form, the mutant ΔSHP-1 was treated with H_2O_2 and IAA and analyzed by MALDI-MS as for the wild-type protein. As expected, the reduced protein showed peptides containing carboxymethylated catalytic (2101 Da) and the remaining backdoor cysteines (1523 Da) (Figure 4A). The sample from the oxidized protein contained a novel peak (3507 Da) representing the peptide containing a disulfide bond between the catalytic (Cys455) and the remaining backdoor (Cys363) cysteines. These data demonstrate the ready formation of a reversible disulfide between the catalytic cysteine and the nearby backdoor cysteine, representing a possible intermediate in the oxidation process of the wild-type protein (Scheme 1).

We next generated the other backdoor cysteine mutant of ΔSHP-1, namely, C363S. (The corresponding C367S mutant of ΔSHP-2 did not express well and could thus not be studied.) Purified C363S showed only a 2-fold reduction in activity as compared to wild-type ΔSHP-1. C363S treated with H_2O_2 as for the wild-type protein showed a similar rate constant for oxidative inactivation (Table 1). Although the nearest backdoor cysteine is absent, the C363S mutant could be rereduced by DTT and GSH with comparable rate constants compared to the wild-type protein, albeit to a lower extent of recovered activity. Peptides identified by MALDI-MS from the oxidized C363S mutant demonstrate that the reversibility of oxidation in the C363S mutant is due to the formation of a disulfide bond between the catalytic (Cys455) and the more distant backdoor (Cys329) cysteines (Figure

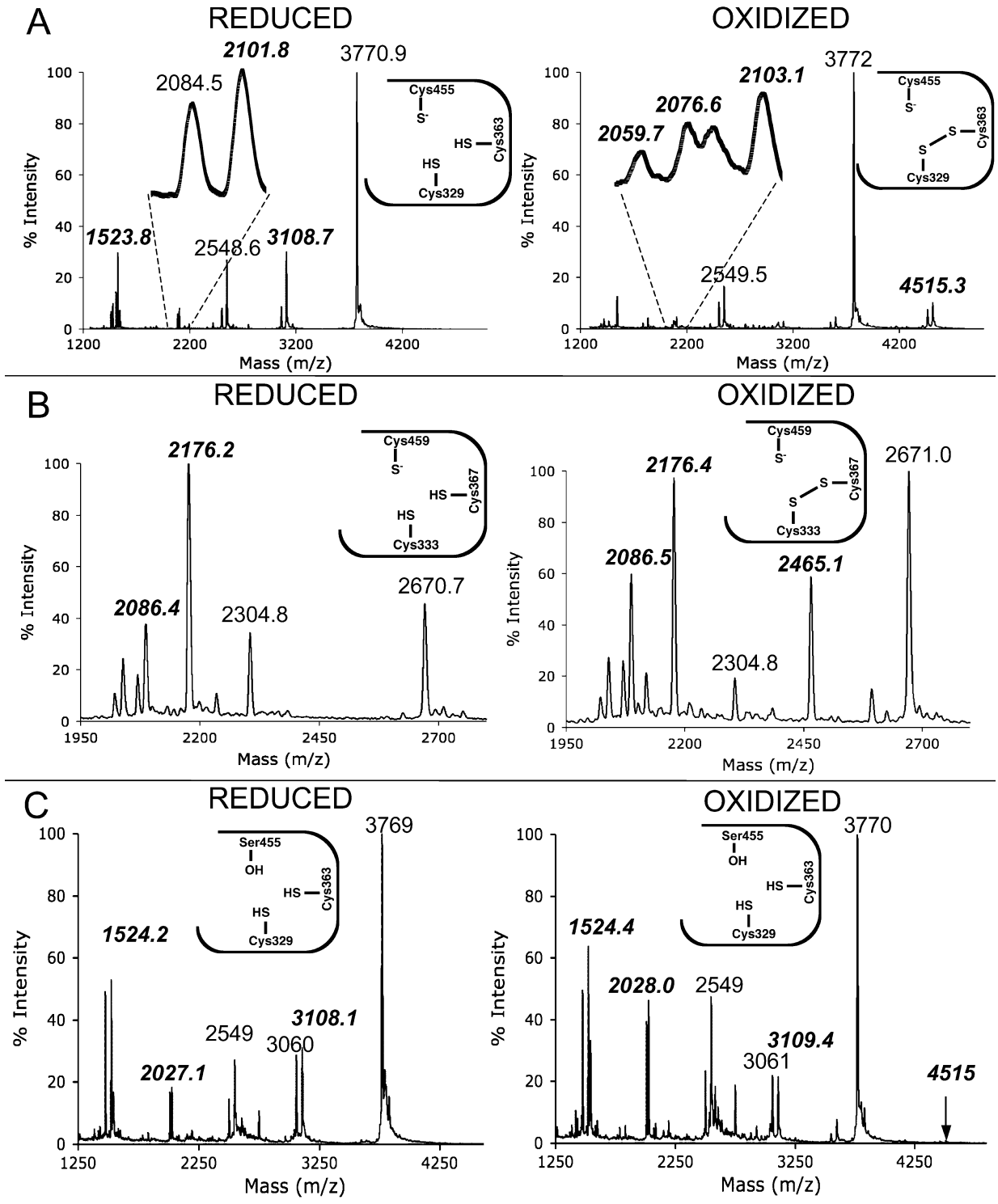

FIGURE 3: MALDI-MS of reduced and oxidized ΔSHP-1 and ΔSHP-2. Wild-type ΔSHP-1, the catalytic mutant C455S of ΔSHP-1, and ΔSHP-2 were untreated (reduced) or treated (oxidized) with H_2O_2 followed by treatment with IAA. Peptide masses containing the catalytic cysteine and the backdoor cysteines are labeled in bold italic type. The schematic insets show the deduced oxidation states of the three cysteines near the active site. (A) The reduced sample from ΔSHP-1 shows the presence of the peptides containing carboxymethylated catalytic cysteine (Cys455, 2101 Da) and the two backdoor cysteines (Cys363, 1523 Da; Cys329, 3108 Da) with a mass increase of 58 Da compared to the unmodified peptides. In the oxidized sample, the two peptides containing the carboxymethylated backdoor cysteines have disappeared, and a larger peptide consistent with formation of a disulfide bond between the two backdoor cysteines is seen instead (4515 Da). The blown-up region shows the active site peptide with the catalytic cysteine in the sulfenic acid (2059 Da) and the sulfinic acid (2076 Da) forms. (B) The reduced sample from ΔSHP-2 shows the carboxymethylated peptide containing the catalytic cysteine (Cys459, 2086 Da) and one of the backdoor cysteines (Cys367, 2176 Da). The mass of the peptide containing the second backdoor cysteine (Cys367) is too small to detect under these MALDI-MS conditions (407 Da). As for ΔSHP-2, the oxidized sample shows the peptide representing the disulfide between the two backdoor cysteines (2465 Da). (C) The reduced sample from the catalytic mutant C455S of ΔSHP-1 shows the presence of the peptides containing the mutated catalytic residue (Ser455, 2027 Da) and the two backdoor cysteines (Cys363, 1523 Da; Cys329, 3108 Da). In contrast to the wild-type protein, the oxidized sample of the mutant still shows the two peptides containing the carboxymethylated backdoor cysteines (compare with panel A) and does not contain the peptide (4515 Da) representing a disulfide bond between the two backdoor cysteines (note arrow at location).

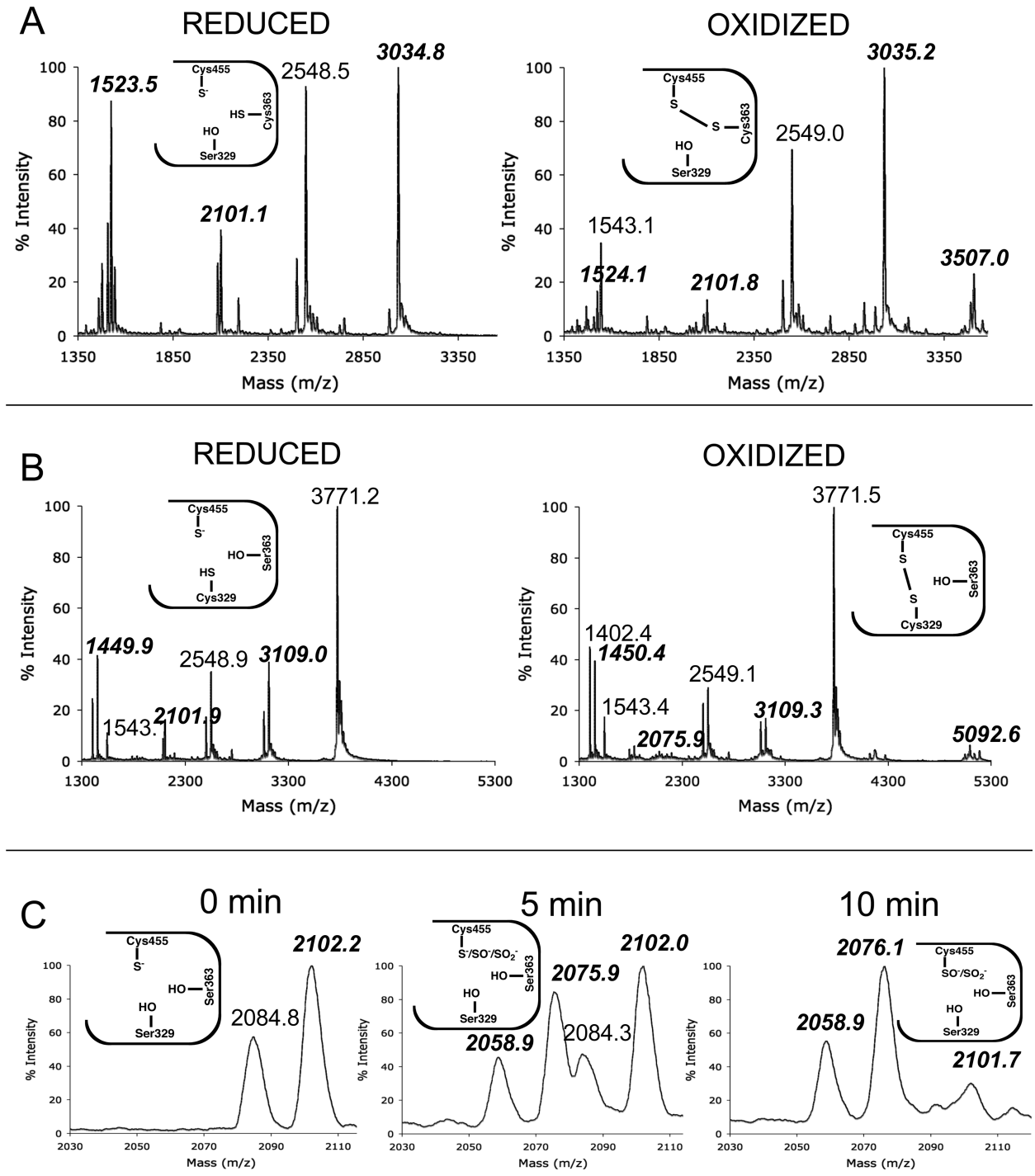

FIGURE 4: MALDI-MS of reduced and oxidized mutants of ΔSHP-1. C329S, C363S, and C329S/C363S mutants of ΔSHP-1 were untreated (reduced) or treated with H_2O_2 (oxidized), followed by IAA treatment. Peptide masses containing the catalytic cysteine and the backdoor cysteines are labeled in bold italic type. The schematic inset shows the deduced oxidation states of the three cysteines near the active site. (A) The C329S mutant. The reduced sample shows the peptides containing the carboxymethylated catalytic cysteine (Cys455, 2101 Da), a carboxymethylated backdoor cysteine (Cys363, 1523 Da), and the backdoor serine mutation (Ser329, 3034 Da). The oxidized sample shows the presence of the peptide containing the disulfide between Cys455 and Cys363 (3507 Da). (B) The C363S mutant. The reduced sample shows the peptides containing carboxymethylated catalytic cysteine (Cys455, 2101 Da), a carboxymethylated backdoor cysteine (Cys329, 3109 Da), and the backdoor serine mutation (Ser363, 1449 Da). The oxidized sample shows the presence of the peptide containing the disulfide between Cys455 and Cys329 (5092 Da) and peptide containing a sulfinic acid-modified catalytic cysteine (2076 Da). (C) The C329S/C363S double mutant. Only the region containing the peptide with catalytic cysteine is shown. The same amount of C329S/C363S was treated with buffer (0 min), 1 mM H_2O_2 for 5 min, or H_2O_2 for 10 min followed by IAA treatment. The fully reduced sample (0 min) shows the peptide containing the carboxymethylated catalytic cysteine (2102 Da). The sulfenic acid- (2058 Da) and the sulfinic acid-modified (2076 Da) cysteines are present in the sample treated with H_2O_2 for 5 min while the 2102 peak representing the unoxidized catalytic cysteine is still dominant. In the sample treated with H_2O_2 for 10 min the peptides containing sulfenic acid- and sulfinic acid-modified cysteine are the major forms present.

4B). The oxidized sample contained a peptide corresponding to this alternative disulfide (5092 Da), whereas the reduced sample showed peptides containing the carboxymethylated catalytic (2101 Da) and more distant backdoor (3109 Da) cysteines. Thus, either of the two backdoor cysteines in ΔSHP-1 can capture the sulfenic acid that arises upon oxidation of the catalytic cysteine (Scheme 1).

The Two Backdoor Cysteines Are Necessary and Sufficient for the Protection of the Catalytic Cysteine. The catalytic domains of both SHP-1 and SHP-2 contain two additional cysteines besides the catalytic and backdoor cysteines. It is theoretically possible that either of these more remote cysteines could also react with the oxidized catalytic cysteine and subsequently exchange to form the more stable backdoor−backdoor cysteine disulfide that we have identified above. Precedence for the involvement of multiple cysteines in the protection of the catalytic cysteine comes from the mitogen-activated protein kinase phosphatase (MKP3) (*34*). To test this possibility, we investigated the properties of the double mutation, eliminating both backdoor cysteines in ΔSHP-1, namely, C329S/C363S. The double mutant protein had a 2-fold decreased activity as compared to the wild-type protein, consistent with the activity seen for the single mutant C363S. The double mutant had a rate constant for oxidization by H_2O_2 that was 9-fold decreased as compared to wild-type ΔSHP-1 (Table 1). Despite a slower oxidation process, treatment of oxidized C329S/C363S with the reductants DTT or GSH did not lead to reactivation, unlike for the wild-type or either single cysteine mutation of ΔSHP-1. In fact, even the mildest possible treatment consistently led to irreversibly oxidized protein. To determine by MALDI-MS the oxidation state of the active site cysteine following inactivation, C329S/C363S was incubated with 1 mM H_2O_2 for 5 min (partial inactivation) or for 10 min (complete inactivation) and analyzed by MALDI-MS. With increasing inactivation, there is an increase in the peptides representing the sulfenic acid- (2059 Da) and sulfinic acid- (2076 Da) modified catalytic cysteine with concomitant loss of the carboxymethylated catalytic cysteine (2102 Da) (Figure 4C). Additionally, no peptides representing disulfide formation with one of the more remote cysteines could be detected (not shown).

DISCUSSION

SHP-1 and SHP-2 are involved in multiple intracellular pathways responding to diverse signals such as integrins, growth factors, cytokines, and hormones. Ligand binding to the various membrane receptors in these pathways not only triggers traditional signaling events inside cells (i.e., phosphorylation, G-protein activation) but also leads to increases in local concentrations of ROS up to 1 mM, thought to be generated in part by the NADPH oxidase system. These concentrations of H_2O_2 are sufficient to oxidize common regulators of these receptors, namely, the PTPs. As we have shown here in vitro, the SHPs are highly susceptible to oxidative inactivation at their active site cysteines, consistent with the identification of the sulfenic acid form of both SHPs upon activation of $CD8^+$ T-cells (*36*) and with previous in vivo data suggesting that oxidation of SHPs plays a regulatory role in signaling (*10*−*13*). Additionally our data provide interesting insights into the kinetic and mechanistic aspects of oxidative SHP regulation.

Kinetically we noted no significant differences in the rates of oxidation and rereduction (by DTT or GSH) between SHP-1 and SHP-2, whether as full-length proteins or as catalytic domains (Table 1). These data are reminiscent of the intriguing similarity in sequence, structure, and activity of these two phosphatases, despite their opposing roles in signal transduction. Clearly, there are aspects of intracellular localization, substrate recognition, and regulation that are insufficiently understood to explain these opposing roles. As a hint toward possible differences between these two phosphatases in their activated form (lacking the inhibitory SH2 domains), we did note that ΔSHP-2 but not ΔSHP-1 could be reactivated by TR/TRR, one of the more likely physiological reductants. Also, although the kinetic rates for reactivation were similar for ΔSHP-1 and ΔSHP-2, the extent of reactivation for ΔSHP-2 was significantly greater than for ΔSHP-1 (Table 1). Whether these data suggest a more permanent inactivation of SHP-1 in response to ROS in comparison to SHP-2 or the involvement of other intracellular reductants remains to be investigated in more detail. An additional hint that the true physiological reductant remains to be identified for both SHPs comes from the measured rates of reduction. In comparison to other PTPs where rates of reactivation have been quantitated, the rereduction of the SHPs is extremely slow. For example, Cdc25 (*17*) and MPK3 (*34*) are reactivated 10−30-fold faster by TR/TRR than ΔSHP-2.

Mechanistically, we have identified a novel end product that protects the oxidation state of the SHPs in a readily reversible form. With the exception of the peroxiredoxins, it is well-known that the higher oxidation states of cysteine (sulfonic and sulfinic acids) are essentially irreversibly oxidized (*37*). Previously known mechanisms for preserving the singly oxidized form of cysteine include the chemically unusual sulfenylamide found in PTP1b and PTPα and the backdoor cysteines found in the low molecular weight and Cdc25 phosphatases, among others. When present in a phosphatase, these backdoor cysteines are highly conserved, suggesting their evolutionary importance to the function and/or regulation of these PTPs. The presence of two highly conserved potential backdoor cysteines in the SHPs raised the possibility that more than one cysteine could serve as a partner for the active site cysteine in the formation of a stable disulfide. Much to our surprise, while such disulfides between the active site cysteine and either of the backdoor cysteines exist as intermediates, the stably oxidized form consists of a reduced catalytic cysteine and a backdoor−backdoor disulfide (Scheme 1). This mechanism is different than the one found in MKP3, where all of the multiple cysteines are involved in disulfides directly with the active site cysteine and do not appear to form disulfides with each other (*34*). This novel oxidized form of the SHPs also emphasizes that identifying oxidized forms of PTPs in vivo must rely on techniques other than trapping sulfenic acids or modified active site cysteines (glutathionylation, disulfides, or sulfenylamides). That is, dissecting redox regulation of PTPs inside cells may be more difficult and complex than previously thought.

Finally, given that the susceptibility to oxidation and the phosphatase activity for PTPs arises from the greatly perturbed pK_as (4−6.5) of the active site cysteines (*38*), the reduced active site cysteines in the stably oxidized form of

the SHPs are most likely returned to a more normal value ($pK_a \sim 9$) in the stably oxidized form of the SHPs. Thus, there exists the expected correlation between oxidation and inactivation, wherein the catalytically essential thiolate is most likely in the thiol form in the oxidized enzyme (Scheme 1). Using X-ray crystallography it may be possible to obtain insights into the local rearrangements within the active site region that allow for a protonated thiol in the oxidized enzyme, as demonstrated by "in crystal" oxidation for the Cdc25B phosphatase (*18*). As shown by the mutagenesis data, a single backdoor cysteine in SHP-1 is sufficient to trap the oxidation of the catalytic cysteine in a reversible state, just as for MKP3. Why the SHPs evolved a mechanism using this novel two-backdoor cysteine trap remains unclear. There may be some advantage for effecting the transfer of oxidizing equivalents to a separate reductant, as seen for example in the complex thiol-transfer reactions of arsenate reductase (*39*) and ribonucleotide reductase (*40*). Establishing the physiologically relevant reductant for the SHPs would allow further probing of this pathway.

In conclusion, we have provided the first in vitro kinetic and mechanistic analysis of redox regulation of the highly homologous SHPs. Despite their opposing roles in the regulation of signaling pathways, we have found the kinetic properties of inactivation and reactivation of SHP-1 and SHP-2 to be highly similar. Most importantly, our discovery of a backdoor−-backdoor disulfide in the presence of a reduced active site cysteine extends the number of different mechanisms by which an oxidized and inactivated PTP can be stabilized in a rereducible form.

REFERENCES

1. Chiarugi, P., and Cirri, P. (2003) Redox regulation of protein tyrosine phosphatases during receptor tyrosine kinase signal transduction. *Trends Biochem. Sci. 28*, 509–514.
2. den Hertog, J., Goren, A., and Wijk, T. (2005) Redox regulation of protein-tyrosine phosphatases. *Arch. Biochem. Biophys. 434*, 11–15.
3. Tonks, N. K. (2005) Redox redux: Revisiting PTPs and the control of cell signaling. *Cell 121*, 667–670.
4. Chiarugi, P., and Buricchi, F. (2007) Protein tyrosine phosphorylation and reversible oxidation: Two cross-talking posttranslation modifications. *Antioxid. Redox Signaling 9*, 1–24.
5. Sundaresan, M., Yu, Z. X., Ferrans, V. J., Irani, K., and Finkel, T. (1995) Requirement for generation of H2O2 for platelet-derived growth factor signal transduction. *Science 270*, 269–299.
6. Heneberg, P., and Draber, P. (2005) Regulation of Cys-based protein tyrosine phosphatases via reactive oxygen and nitrogen species in mast cells and basophils. *Curr. Med. Chem. 12*, 1859–1871.
7. Neel, B. G., and Tonks, N. K. (1997) Protein tyrosine phosphatases in signal transduction. *Curr. Opin. Cell Biol. 9*, 193–204.
8. Feng, G.-S. (1999) Shp-2 tyrosine phosphatase: signaling one cell or many. *Exp. Cell Res. 253*, 47–54.
9. Neel, B. G., Gu, H., and Pao, L. (2003) The "Shp"ing news: SH2 domain-containing tyrosine phosphatases in cell signaling. *Trends Biochem. Sci. 28*, 284–293.
10. Lee, K., and Esselmann, W. J. (2002) Inhibition of PTPs by H(2)O(2) regulates the activation of distinct MAPK pathways. *Free Radical Biol. Med. 33*, 1121–1132.
11. Kwon, J., Qu, C.-K., Maeng, J.-S., Falahati, R., Lee, C., and Williams, M. S. (2005) Receptor-stimulated oxidation of SHP-2 promotes T-cell adhesion through SLP-76-ADAP. *EMBO J. 24*, 2331–2341.
12. Meng, T.-C., Fukada, T., and Tonks, N. K. (2002) Reversible oxidation and inactivation of protein tyrosine phosphatases in vivo. *Mol. Cell 9*, 387–399.
13. Chen, C.-H., Cheng, T.-H., Lin, H., Shih, N.-L., Chen, Y.-L., Chen, Y.-S., Cheng, C.-F., Lian, W.-S., Meng, T.-C., Chiu, W.-T., and Chen, J.-J. (2006) Reactive oxygen species generation is involved in epidermal growth factor receptor transactivation through the transient oxidization of SHP-2 in endothelin-1 signaling pathway in rat cardiac fibroblasts. *Mol. Pharmacol. 69*, 1347–1355.
14. Dillet, V., Van Etten, R. L., and Bashford, D. (2000) Stabilization of charges and protonation states in the active site of the protein tyrosine phosphatases: A computational study. *J. Phys. Chem. B 104*, 11321–11333.
15. Chiarugi, P. (2001) The redox regulation of LMW-PTP during cell proliferation or growth inhibition. *IUMBM Life 52*, 55–59.
16. Savitsky, P. A., and Finkel, T. (2002) Redox regulation of Cdc25C. *J. Biol. Chem. 277*, 20535–20540.
17. Sohn, J., and Rudolph, J. (2003) Catalytic and chemical competence of regulation of Cdc25 phosphatase by oxidation/reduction. *Biochemistry 42*, 10060–10070.
18. Buhrman, G., Parker, B., Sohn, J., Rudolph, J., and Mattos, C. (2005) Structural mechanism of oxidative regulation of the phosphatase Cdc25B via an intramolecular disulfide bond. *Biochemistry 44*, 5307–5316.
19. Rudolph, J. (2005) Redox regulation of the Cdc25 phosphatases. *Antioxid. Redox Signaling 7*, 761–767.
20. Kwon, J., Lee, S.-R., Yang, K.-S., Ahn, Y., Kim, Y. J., Stadtman, E. R., and Rhee, S. G. (2004) Reversible oxidation and inactivation of the tumor suppressor PTEN in cells stimulated with peptide growth factors. *Proc. Natl. Acad. Sci. U.S.A. 101*, 16419–16424.
21. Song, H., Hanlon, N., Brown, N. R., Noble, M. E. M., Johnson, L. N., and Barford, D. (2001) Phosphoprotein-protein interactions revealed by the crystal structure of kinase-associated phosphatase in complex with phospho-Cdk2. *Mol. Cell 7*, 615–626.
22. Salmeen, A., Andersen, J. N., Myers, M. P., Meng, T.-C., Hinks, J. A., Tonks, N. K., and Barford, D. (2003) Redox regulation of protein tyrosine phosphatase 1B involves a sulphenyl-amide intermediate. *Nature 423*, 769–773.
23. van Montfort, R. L. M., Congreve, M., Tisi, D., Carr, R., and Jhoti, H. (2003) Oxidation state of the active site cysteine in protein tyrosine phosphatase 1B. *Nature 423*, 773–777.
24. Yang, J., Groen, A., Lemeer, S., Jans, A., Slijper, M., Roe, S. M., den Hertog, J., and Barford, D. (2007) Reversible oxidation of the membrane distal domain of receptor PTPalpha is mediated by a cyclic sulfenamid. *Biochemistry 46*, 709–719.
25. Pregel, M. J., and Storer, A. C. (1997) Active site titration of the tyrosine phosphatases SHP-1 and PTP1B using aromatic disulfides. *J. Biol. Chem. 272*, 23552–23558.
26. Barrett, D. M., Black, S. M., Todor, H., Schmidt-Ullrich, R. K., Dawson, K. S., and Mikkelsen, R. B. (2005) Inhibition of protein-tyrosine phosphatase my mild oxidative stress is dependent on S-nitrosylation. *J. Biol. Chem. 280*, 14453–14461.
27. Yang, J., Liang, X. S., Niu, T. Q., Meng, W. Y., Zhao, Z. Z., and Zhou, G. W. (1998) Crystal structure of the catalytic domain of protein-tyrosine phosphatase SHP-1. *J. Biol. Chem. 273*, 28199–28207.
28. Hof, P., Pluskey, S., Dhe-Paganon, S., Eck, M. J., and Shoelson, S. E. (1998) Crystal structure of the tyrosine phosphatase SHP-2. *Cell 92*, 441–450.
29. Cunnick, J. M., Dorsey, J. F., Mei, L., and Wu, J. (1998) Reversible regulation of Shp-1 tyrosine phosphatase activity by oxidation. *Biochem. Mol. Biol. Int. 45*, 887–894.
30. Sugimoto, S., Lechleider, R. J., Shoelson, S. E., Neel, B. G., and Walsh, C. T. (1993) Expression, purification, and characterization of SH2-containing protein tyrosine phosphatase, SH-PTP2. *J. Biol. Chem. 268*, 22771–22776.
31. Sugimoto, S., Wandless, T. J., Shoelson, S. E., Neel, B. G., and Walsh, C. T. (1994) Activation of the SH2-containing protein tyrosine phosphatase, SH-PTP2, by phosphotyrosine-containing peptides derived from insulin receptor substrate-1. *J. Biol. Chem. 269*, 13614–13622.
32. Wang, J., and Walsh, C. T. (1997) Mechanistic studies on full length and the catalytic domain of the tandem SH2 domain-containing protein tyrosine phosphatase: analysis of phosphoenzyme levels and Vmax stimulatory effects of glycerol and of a phosphotyrosyl peptide ligand. *Biochemistry 36*, 2993–2999.
33. Denu, J. M., and Tanner, K. G. (1998) Specific and reversible inactivation of protein tyrosine phosphatases by hydrogen peroxide: Evidence for a sulfenic acid intermediate and implication for redox regulation. *Biochemistry 37*, 5633–5642.
34. Seth, D., and Rudolph, J. (2006) Redox regulation of Map kinase phosphatase 3. *Biochemistry 45*, 8476–8487.

35. Claiborne, A., Yeh, J. I., Mallett, T. C., Luba, J., Crane, E. J., Charrier, V., and Parsonage, D. (1999) Protein-sulfenic acids: diverse roles for an unlikely player in enzyme catalysis and redox regulation. *Biochemistry 38*, 15407–15416.
36. Michalek, R. D., Nelson, K. J., Holbrook, B. C., Yi, J. S., Stridiron, D., Daniel, L. W., Fetrow, J. S., King, S. B., Poole, L. B., and Grayson, J. M. (2007) The requirement of reversible cysteine sulfenic acid formation for T cell activation and function. *J. Immunol. 179*, 6456–6467.
37. Woo, H. A., Chae, H. Z., Hwang, S. C., Yang, K.-S., Kang, S. W., Kim, K., and Rhee, S. G. (2003) Reversing the inactivation of peroxiredoxins caused by cysteine sulfinic acid formation. *Science 300*, 653–656.
38. Peters, G. H., Frimurer, T. M., and Olsen, O. H. (1998) Electrostatic evaluation of the signature motif (H/V)CX5R(S/T) in protein-tyrosine phosphatases. *Biochemistry 37*, 5383–5393.
39. Messens, J., Martins, J. C., Van Belle, K., Brosens, E., Desmyter, A., De Gieter, M., Wieruszeski, J.-M., Willem, R., Wyns, L., and Zegers, I. (2002) All intermediates of the arsenate reductase mechanism, including an intramolecular dynamic disulfide cascade. *Proc. Natl. Acad. Sci. U.S.A. 99*, 8506–8511.
40. Stubbe, J., and van der Donk, W. A. (1995) Ribonucleotide reductases: radical enzymes with suicidal tendencies. *Chem. Biol. 2*, 793–801.

BI801973Z